Formation Configuration for Cooperative Multiple UAV Via Backstepping PID Controller

Conference Paper · September 2018

DOI: 10.2514/6.2018-5282

Ahmed Taimour Hafez
Military Technical College

Mahmoud Ashry
Military technical college, Cairo, egypt

Gamal Elnashar
Military Technical College

AIAA SPACE Forum
17-19 September 2018, Orlando, FL
2018 AIAA SPACE and Astronautics Forum and Exposition

10.2514/6.2018-5282

Formation Configuration for Cooperative Multiple UAV via Backstepping PID Controller

M. Mahfouz[1], Ahmed Taimour Hafez[2], M. Ashry[3], and G. Elnashar[4]
Military Technical College, 11766 Cairo, Egypt

The issue of formation rearrangement for a troop of cooperative unmanned vertical take-off and landing (VTOL) aircrafts in an obstacle-loaded atmosphere is figured out using a purposed backstepping based proportional–integral–derivative controller (PID). The designed controller is developed to regulate every unmanned quadrotor within the troop in an exceedingly localized manner guaranteeing the reserving of the required geometric formation. The backstepping technique could be a promising control technique for nonlinear and coupled multivariable systems. The essential contribution in this paper concentrates on resolving the formation issue for a troop of cooperative pilotless VTOL airplanes in a decentralized manner via backstepping PID regulator. The designed decentralized controller guarantees the success of the required mission of the swarming troop. The simulation results declare the successes of the proposed controller in guaranteeing the stability of the system and reserving of the desired geometric formation either within the existence or absence of obstacles.

I. Introduction

In recent decenniums, unmanned aerial vehicles (UAVs) have charged a mature concern with their success among achieving heaps of progress in several applications in each military and civilian scopes [1-3]. The UAV is characterized by its capacity to accomplish its assignments in alleged "D-cube" operations (Dull – Dangerous-Dirty) atmosphere with no risk for manned pilots resources [4, 5], easy to preserve and low worth. Therefore, UAV has attained growing concern from scientists, researchers, and engineers. UAVs may be thought about as a hopeful alternative for numerous pilotless military and civilian exercises [6-8].

The auspicious results of a single UAV in executing varied applications persuade the utilization of multiple UAVs cooperating collectively to meet the required tasks [9-11]. Cooperative UAVs guarantees the success of the desired missions with better performance compared with single UAV [12-15].

Certain strategies are needed for multiple cooperative UAVs to cooperate collectively to fulfill the required goals. These strategies which defined by the cooperative UAVs attributes are known as UAVs tactics. These tactics can be classified into the swarming, mission duty, structure rearrangement, and active blockade [16, 17].

Formation rearrangement is outlined by the power of the multiple cooperative UAVs to preserve a desired geometric structure [12], and reconfigure to a different formation per the surrounding circumstances guaranteeing the success of the required application [16, 18]. Each member in the cooperative UAV troop must respect Reynold's rules of flocking during its formation [19-21]. Each UAV member has to match its velocity and separating distance from its neighbors and avoid colliding with its neighbors or obstacles [22]. There are several varieties of controls in the formation rearrangement of multiple cooperative UAVs domain. The scope of these control techniques steadily growing fast last decade including hybrid divergence particle swarm optimization (PSO) and time optimal orientation tactic to a troop of UAVs in 2009 [23], genetic algorithm and hybrid molecule swarm optimization in 2013 [24], optimal formation control in 2015 [25], fault-tolerant cooperative control in 2016 [26, 27], distributed

[1] Ph.D. Student, Department of Electrical Engineering, MTC, Cairo, Egypt; m.mahfouz.trc@gmail.com.
[2] Ahmed T. Hafez is with the Department of Electrical Engineering, MTC, Cairo, Egypt; a.taimour@mtc.edu.eg
[3] Head of Optoelectronics and control department, MTC, Cairo, Egypt. mmaashry@mtc.edu.eg
[4] Dean of MTC, Cairo, Egypt. g.elnshar@mtc.edu.eg

cooperative control based on unanimity called Consensus theory [28], and optimal control of formation rearrangement for a troop of UAVs founded on Legendre Pseudospectral hypothesis in 2017 [29].

One of the ultimate remarkable kind of UAVs in duration is the four rotor VTOL aircraft named as quadrotor [30, 31]. Some of its useful features are its competence of maneuverability and ease of design and maintain leading that VTOL aircraft has superiority over conventional aircraft [32-37]. Unlike the traditional vertical takeoff vehicles, the quadrotors are characterized by a plain framework and minimum cost [32]. However, the complexity of controlling the quadrotors during autonomous hovering and maneuver has become a great challenge for engineers due to its nonlinearities and coupled variables [38].

The main contribution of this paper concentrates in solving the formation problem for a troop of cooperative VTOLs using a designed backstepping based proportional–integral–derivative controller (PID). Most backstepping controller used as an upper hand controller [39-42]; however the proposed controller is implemented to control each quadrotor in a decentralized pattern. The proposed designed controller has the notability to handle the under-actuated properties and the nonlinearities of the quadrotors. It is shown that controlling each quadrotor independently guarantees more stability and robustness of the complete formation of the troop.

The backstepping technique is a well-chosen control technique for highly nonlinear systems [2, 3, 36, 39-49]. Backstepping methodology putts the whole controller decomposition into several steps to be completed. In each designing step, a virtual control is selected to make the prior system stable. Consequently, the control algorithm is modified gradually until the system achieves stable control effect [50]. The adaptability of the backstepping technique lies in its recursive process of Lyapunov functions. The backstepping selects recursive convenient variables as implicit inputs for reduced range subsystems of the complete system. The Lyapunov functions are planned for every steady implicit controller guaranteeing the fastness of the entire control system [51]. The advantages of backstepping techniques are that the controller has fast convergence rate and has the ability to deal with nonlinear systems likewise the effect of outside uncertainty and stabilize the whole system to be able to drive a quadrotor to the desired trajectory [3], while bad system robustness can be considered as the central disadvantage of this way [50]. The underlying controller is established on the restitution of the Coriolis and gyroscopic torques and the exercise of a PD framework for altitude and yaw scopes along with the exercise of backstepping regulator primarily for the circular control, where the relative process outlined the Euler angles terms and the derivative process outlined the airframe angular velocity terms. After that optimization method is used to obtain the appropriate parameters quantities.

This paper is arranged as follows; Section II symbolizes the mathematical model of the VTOL understudy, whilst Section III represents the backstepping PID controller layout. The simulation results of trajectory tracking using the proposed backstepping controller for cooperative VTOLs in free and obstacle-loaded atmosphere are represented in Section IV. Furthermore, a collision avoidance innovation is granted in section IV. Finally, the current work is summarized and some of the outlook intentions are highlighted in Section V.

II. Quadrotor Framework Paradigm

Quadrotor composed of four rotors mounted at an equivalent separation from the focal hub in a uniformed pattern. The whole rotors are adjusted to produce thrust and torque. Each rotor of the quadrotor generates both thrust and torque. The anterior and posterior rotors spin counter-clockwise (produce clockwise torque) whereas the opposite couple spin clockwise to stabilize the aggregate torque of the whole system. So, we can stabilize the quadrotor by adjusting the rotor speed of each one separately. Assume that t_n is the thrust and q_n is the torque to n_{th} rotor, where $n = 1, 2, 3, 4$. These amounts are charged by quadrotor mass and moment of inertia. Announcing the space of the rotor from the middle of mass by d, a series of four control datum U_n can be inserted as a function of normalized particular thrusts and torques as in the coming after equations. The overall thrust, roll, pitch, and yaw moments are presented in (1), (2), (3), and (4) respectively.

$$U_1 = t_1 + t_2 + t_3 + t_4 \tag{1}$$

$$U_2 = d(t_3 - t_4) \tag{2}$$

$$U_3 = d(t_1 - t_2) \tag{3}$$

$$U_4 = q_1 + q_2 - q_3 - q_4 \tag{4}$$

The technique of modeling the quadrotor does not seem like the one that exercised for fixed wing UAVs. Actually, the circular conversions are not executed in the same configuration to set out from the earth to the body frame. Normally, the most powerful way is to carry out the eventual turnover of the earth framework to the body conversion straight with the thrust part [52]. So, for the body to earth transformation, the subsequent direction cosine matrix is counted as in (5) [31, 37, 53].

$$R_{zxy}=\begin{bmatrix}\cos\theta\cos\psi+\sin\theta\sin\psi\sin\phi & \sin\theta\sin\phi\cos\psi-\cos\theta\sin\psi & \sin\theta\cos\phi\\ \cos\phi\sin\psi & \cos\psi\cos\phi & -\sin\phi\\ \cos\theta\sin\psi\sin\phi-\sin\theta\cos\psi & \cos\theta\sin\phi\cos\psi+\sin\theta\sin\psi & \cos\theta\cos\phi\end{bmatrix} \tag{5}$$

Whereas: ϕ,θ,ψ Roll, Pitch, and Yaw angularities respectively.

A Newtonian modeling way was selected to determine the quadrotor dynamics for control objectives. The Newtonian way is the ultimate favorable choice for modeling solid bodies in six degrees of freedom [54, 55]. Eventually, the Newtonian founded equations applied to fetch a robust frame in 6-degrees of freedom are clarified and can be found in many references [55, 56]. The dynamics of a rigid body under outer forces utilized to the midpoint of mass and declared in the body-fixed frame are in Newton-Euler formalism given in (6) [31, 37, 53, 57].

$$\begin{aligned} m\dot{q}^b+\omega^b\times mq^b &= F^b\\ I\,\dot{\omega}^b+\omega^b\times I\,\omega^b &= t^b \end{aligned} \tag{6}$$

Suppose a steady earth scope E and a steady body scope B as shown in Fig. (1). Utilizing Euler angles characteristics; the airframe bearing in space is determined by a rotation R from B to E whereas $R\in SO3$ are the rotation matrix.

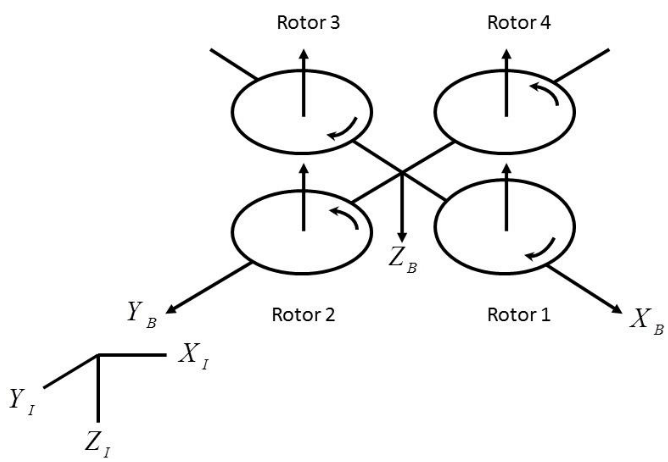

Fig. 1 Quadrotor composition, scope system with a body set scope B and an inertial scope I.

Dynamics of a solid frame under outer forces utilized to the midpoint of mass and declared in the body-steady scope are in Newton-Euler approach given in (7) [31, 37, 58-60].

$$\begin{aligned}
\ddot{x} &= \frac{1}{m}\left[\left(\sin\theta\cos\phi\cos\psi+\sin\phi\sin\psi\right)\sum_{n=1}^{4}T_n-\sum_{n=1}^{4}H_{xn}-\tfrac{1}{2}\rho A_c C_x\dot{x}\left|\dot{x}\right|\right]\\
\ddot{y} &= \frac{1}{m}\left[\left(\sin\theta\cos\phi\sin\psi-\sin\phi\cos\psi\right)\sum_{n=1}^{4}T_n-\sum_{n=1}^{4}H_{yn}-\tfrac{1}{2}\rho A_c C_y\dot{y}\left|\dot{y}\right|\right]\\
\ddot{z} &= \frac{1}{m}\left[mg-\left(\cos\phi\cos\psi\right)\sum_{n=1}^{4}T_n\right]\\
\ddot{\theta} &= \frac{1}{I_{yy}}\left[\dot{\phi}\dot{\psi}\left(I_{zz}-I_{xx}\right)+\Omega_r J_r\dot{\phi}+l\left(T_1-T_3\right)+h\sum_{n=1}^{4}H_{xn}+(-1)^{n+1}\sum_{n=1}^{4}R_{myn}\right]\\
\ddot{\phi} &= \frac{1}{I_{xx}}\left[\dot{\theta}\dot{\psi}\left(I_{yy}-I_{zz}\right)+\Omega_r J_r\dot{\theta}+l\left(-T_2+T_4\right)-h\sum_{n=1}^{4}H_{yn}+(-1)^{n+1}\sum_{n=1}^{4}R_{mxn}\right]\\
\ddot{\psi} &= \frac{1}{I_{zz}}\left[\dot{\phi}\dot{\theta}\left(I_{xx}-I_{yy}\right)+\Omega_r J_r+(-1)^{n}\sum_{n=1}^{4}Q_n+l\left(H_{x2}-H_{x4}\right)+l\left(-H_{y1}+H_{y3}\right)\right]
\end{aligned} \tag{7}$$

III. Backstepping Controller Design

The backstepping PID regulator fetches the data from the sensors straight with the assigned mission as inputs. The controller uses during the calculation many parameters, which represent the states and the dynamics of the quadrotors. The output of the algorithm is the code that allocates the PWM signal for each motor of the four motors of each quadrotor.

Backstepping PID control is selected to provide circular control of the i_{th} quadrotor airplane in which the inputs U_{2i} , U_{3i} and U_{4i} control quadrotor aerial robot at hovering, where $i = 1, 2, ..., j$ (j is the number of quadrotor in the swarming troop).

At the 1st step, the pitch pursuit error is resolved as in (8), the error which associated with the translational position is assumed as the difference value between the current and the required path.

$$e_i = \theta_i - \theta_{di} \tag{8}$$

Where θ_{di} is a desired pitch angle trajectory for i_{th} quadrotor.

Differentiating Eq. (8), the dynamics of this error are acquired as in (9):

$$\dot{e}_i = \dot{\theta}_i - \dot{\theta}_{di} \tag{9}$$

The 1st error in the controller design will be:

$$\chi_{1i} = k_{1i} e_i + k_{2i} \int e_i dt \tag{10}$$

Where k_{1i} and k_{2i} are positive setting parameters and the 2nd side at the right-hand half stands for the roll error.

Selecting the 1st Lyapunov exercise positive definite as in (11):

$$V_{1i} = \tfrac{1}{2} \chi_{1i}^2 \tag{11}$$

Differentiating Eq. (11) yield:

$$\begin{aligned} \dot{V}_{1i} &= \chi_{1i} \dot{\chi}_{1i} = \chi_{1i} (k_{1i} \dot{e}_i + k_{2i} e_i) \\ &= \chi_{1i} (k_{1i} \dot{\theta}_i - k_{1i} \dot{\theta}_{di} + k_{2i} e_i) \end{aligned} \tag{12}$$

Assuming $\dot{\theta}_i$ be the virtual control, the desired virtual control $(\dot{\theta})_{di}$ is characterized as in (13):

$$(\dot{\theta})_{di} = \dot{\theta}_{di} - \frac{k_{2i}}{k_{1i}} e_i - \frac{c_{1i} \chi_{1i}}{k_{1i}} \tag{13}$$

Where c_1 is positive constant to accelerate the pitch velocity tracking loop.

For the 2nd step, the virtual control $\dot{\theta}_i$ is determining the pitch value of the underlying quadrotors and its own errors also, that is given as in (14):

$$\chi_{2i} = \dot{\theta}_i - (\dot{\theta})_{di} = \dot{\theta}_i - \dot{\theta}_{di} + \frac{k_{2i}}{k_{1i}} e_i + \frac{c_{1i} \chi_{1i}}{k_{1i}} \tag{14}$$

From Eq. (9): e_{2i} can be rephrased as in (15):

$$\chi_{2i} = \dot{e}_i + \frac{k_{2i}}{k_{1i}} e_i + \frac{c_{1i} \chi_{1i}}{k_{1i}} = \frac{1}{k_{1i}} (k_{1i} \dot{e}_i + k_{2i} e_i + c_{1i} \chi_{1i}) \tag{15}$$

Integrating Eq. (10) yields:

$$\dot{\chi}_{1i} = k_{1i} \dot{e}_i + k_{2i} e_i \tag{16}$$

Substituting $\dot{e}_{1i}$ from Eq. (16) into Eq. (15) yields:

$$\chi_{2i} = \frac{1}{k_{1i}} (\dot{\chi}_{1i} + c_{1i} \chi_{1i}) \tag{17}$$

Choosing the 2nd Lyapunov function positive definite as in (18):

$$V_{2i} = \tfrac{1}{2} (\chi_{1i}^2 + \chi_{2i}^2) \tag{18}$$

Integrating Eq. (18) yields:

$$\dot{V}_{2i} = \chi_{1i}\dot{\chi}_{1i} + \chi_{2i}\dot{\chi}_{2i} \tag{19}$$

Substituting $\dot{e}_{1i}$ and $\dot{e}_{2i}$ from Eq. (16) and Eq. (17) into Eq. (19) yields:

$$\begin{aligned}\dot{V}_{2i} &= \chi_{2i}\left[\left(k_{1i}^2 + \frac{c_{1i}k_{2i}}{k_{1i}}\right)e_i + \left(c_{1i} + \frac{k_{2i}}{k_{1i}}\right)\dot{e}_i + k_{1i}k_{2i}\int e_i dt + \left(\frac{I_{zi} - I_{xi}}{I_{yi}}\right)\dot{\phi}_i\dot{\psi}_i + \frac{l}{I_{yi}}u_{2i} - \ddot{\phi}_{di}\right] \\ &\quad - \chi_{1i}\left[c_{1i}k_{1i}e_i + c_{1i}k_{2i}\int e_i dt\right]\end{aligned} \tag{20}$$

The wanted dynamics are:

$$\begin{aligned}\dot{V}_{2i} &= -\frac{c_{2i}}{k_{1i}}[\dot{\chi}_{1i} + c_{1i}\chi_{1i}] \\ &= -(c_{2i})\dot{e}_i - (\alpha_i)e_i - (\beta_i)\int e_i dt\end{aligned} \tag{21}$$

Where c_{2i} , $\alpha_i = \left(c_{1i}c_{2i} + \frac{c_{2i}k_{2i}}{k_{1i}}\right)$, and $\beta_i = \left(\frac{c_{1i}c_{2i}k_{2i}}{k_{1i}}\right)$ are positive tuning parameters.

The desired control U_{2i} is identified as:

$$\begin{aligned}U_{2i} = \frac{I_{yi}}{l}\Bigg[&-\left(k_{1i}^2 + \frac{c_{1i}k_{2i}}{k_{1i}} + c_{1i}c_{2i} + \frac{c_{2i}k_{2i}}{k_{1i}}\right)e_i - \left(c_{1i} + \frac{k_{2i}}{k_{1i}} + c_{2i}\right)\dot{e}_i - \left(\frac{I_{zi} - I_{xi}}{I_{yi}}\right)\dot{\phi}_i\dot{\psi}_i \\ &- \left(k_{1i}k_{2i} + \frac{c_{1i}c_{2i}k_{2i}}{k_{1i}}\right)\int e_i dt + \ddot{\phi}_{di}\Bigg]\end{aligned} \tag{22}$$

From (22), U_{2i} is a backstepping PID control and its gains are:

$$K_{Pi} = \left(k_{1i}^2 + \frac{c_{1i}k_{2i}}{k_{1i}} + c_{1i}c_{2i} + \frac{c_{2i}k_{2i}}{k_{1i}}\right), K_{Ii} = \left(k_{1i}k_{2i} + \frac{c_{1i}c_{2i}k_{2i}}{k_{1i}}\right), \text{and } K_{Di} = \left(c_{1i} + \frac{k_{2i}}{k_{1i}} + c_{2i}\right) \tag{23}$$

In the same way we can obtain U_{3i} and U_{4i} as in Eq. (24) and Eq. (25):

$$\begin{aligned}U_{3i} = \frac{I_{xi}}{l}\Bigg[&-\left(k_{3i}^2 + \frac{c_{3i}k_{4i}}{k_{3i}} + c_{3i}c_{4i} + \frac{c_{4i}k_{4i}}{k_{3i}}\right)e_i - \left(c_{3i} + \frac{k_{4i}}{k_{3i}} + c_{4i}\right)\dot{e}_i - \left(\frac{I_{yi} - I_{zi}}{I_{xi}}\right)\dot{\theta}_i\dot{\psi}_i \\ &- \left(k_{3i}k_{4i} + \frac{c_{3i}c_{4i}k_{4i}}{k_{3i}}\right)\int e_i dt + \ddot{\theta}_{di}\Bigg]\end{aligned} \tag{24}$$

$$U_{4i} = \frac{I_{zi}}{l}\left[-\left(k_{5i}^2 + \frac{c_{5i}k_{6i}}{k_{5i}} + c_{5i}c_{6i} + \frac{c_{6i}k_{6i}}{k_{5i}}\right)e_i - \left(k_{5i}k_{6i} + \frac{c_{5i}c_{6i}k_{6i}}{k_{5i}}\right)\int e_i dt - \left(c_{5i} + \frac{k_{6i}}{k_{5i}} + c_{6i}\right)\dot{e}_i + \ddot{\psi}_{di}\right] \tag{25}$$

IV. Simulation Results

Concerning approving the offered control approaches, a simulation environment is settled under "Simulink-Matlab”. The simulation is established on the complete nonlinear model of the quadrotors introduced by the movement equations introduced in Eq. (7). The simulation results recorded in the occupancy and absence of obstacles as well, so the simulation results will be presented in both an obstacle-free atmosphere and an obstacle-loaded atmosphere.

A. Obstacle-Free Atmosphere:

The simulation results are introduced for a troop of three cooperative quadrotors initially started from different operating points and converging to a desired position respecting the separating distance. The paths of the leader UAV through X-axis, Y-axis and Z-axis are presented in Figs. (2), (3) and (4), respectively. The path trajectory is presented as different step inputs then inhomogeneous parabolic path. The reference trajectory used to evaluate the position controllers. Fig. (5) represents the trajectory of the cooperative UAV troop following the desired path in 2-D, while the trajectory in 3-D is represented in Fig.(6).

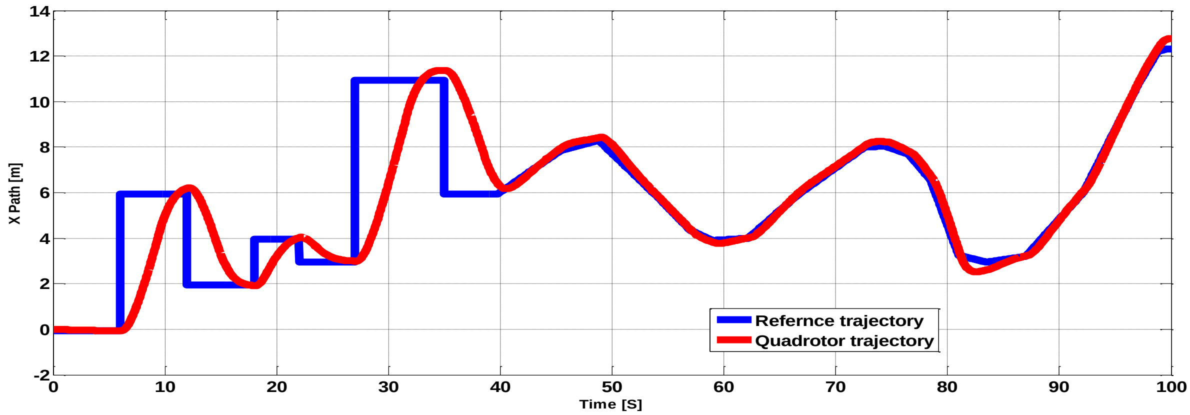

Fig. 2 The path of the elementary quadrotor in the X-axis.

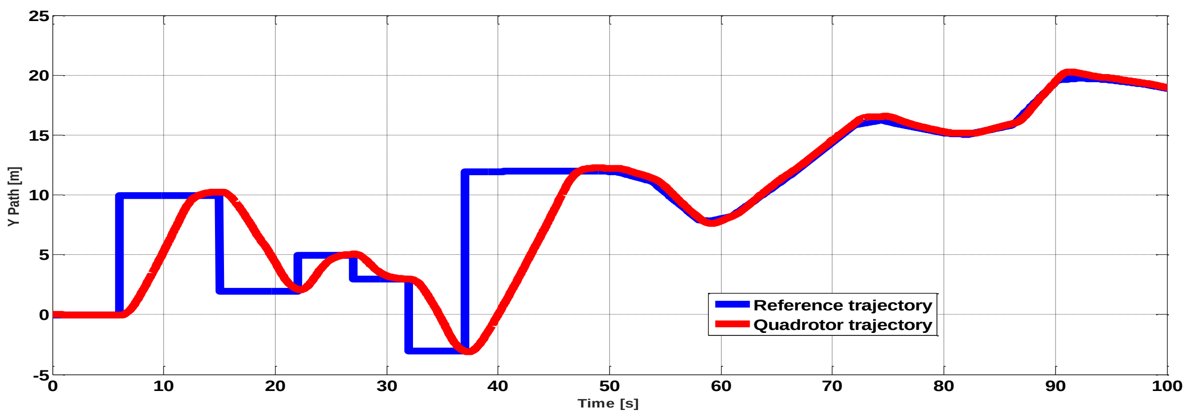

Fig. 3 The path of the elementary quadrotor in the Y-axis.

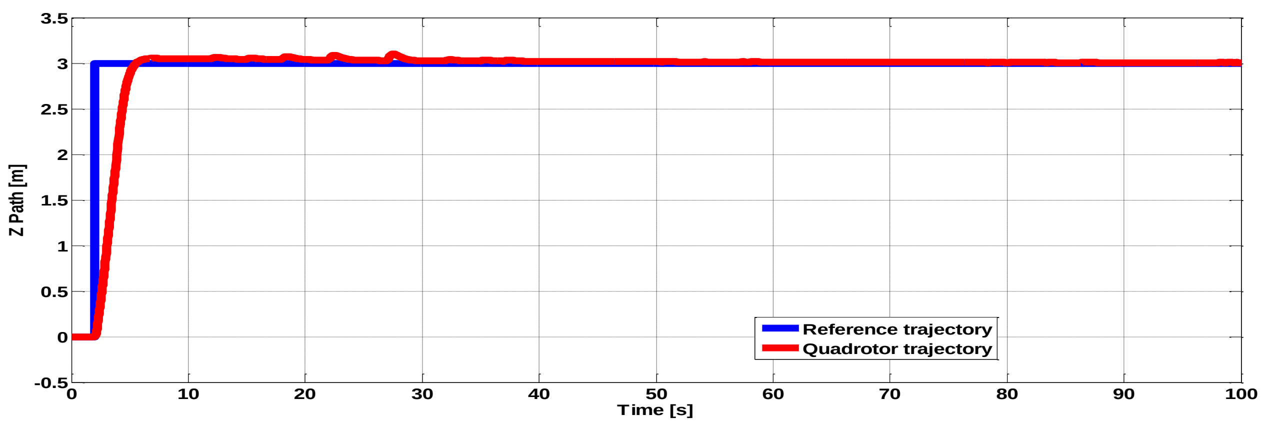

Fig. 4 The path of the elementary quadrotor in the Z-axis.

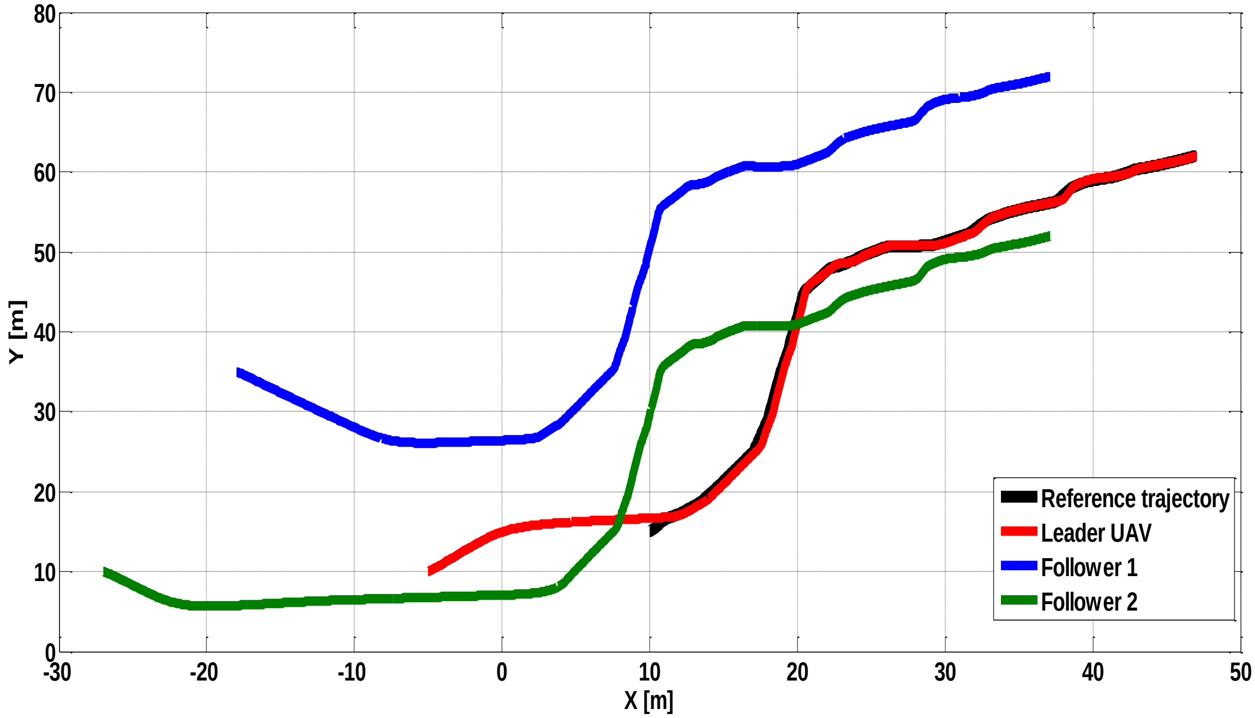

Fig. 5 The path of the UAV troop following the desired trajectory in 2-D.

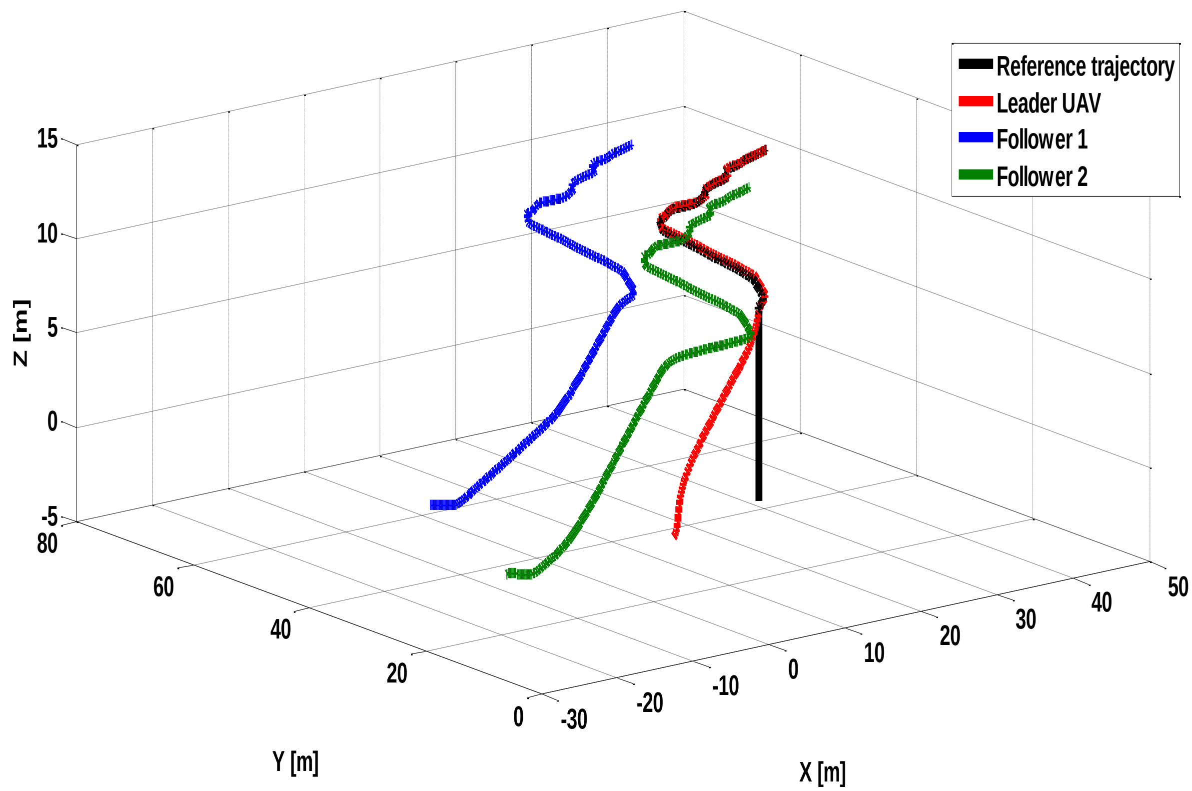

Fig. 6 The path of the UAV troop following the desired trajectory in 3-D.

The detaching distances among the leader UAV and the two followers in the X and Y pivots are shown in Fig. (7) and Fig. (8), respectively.

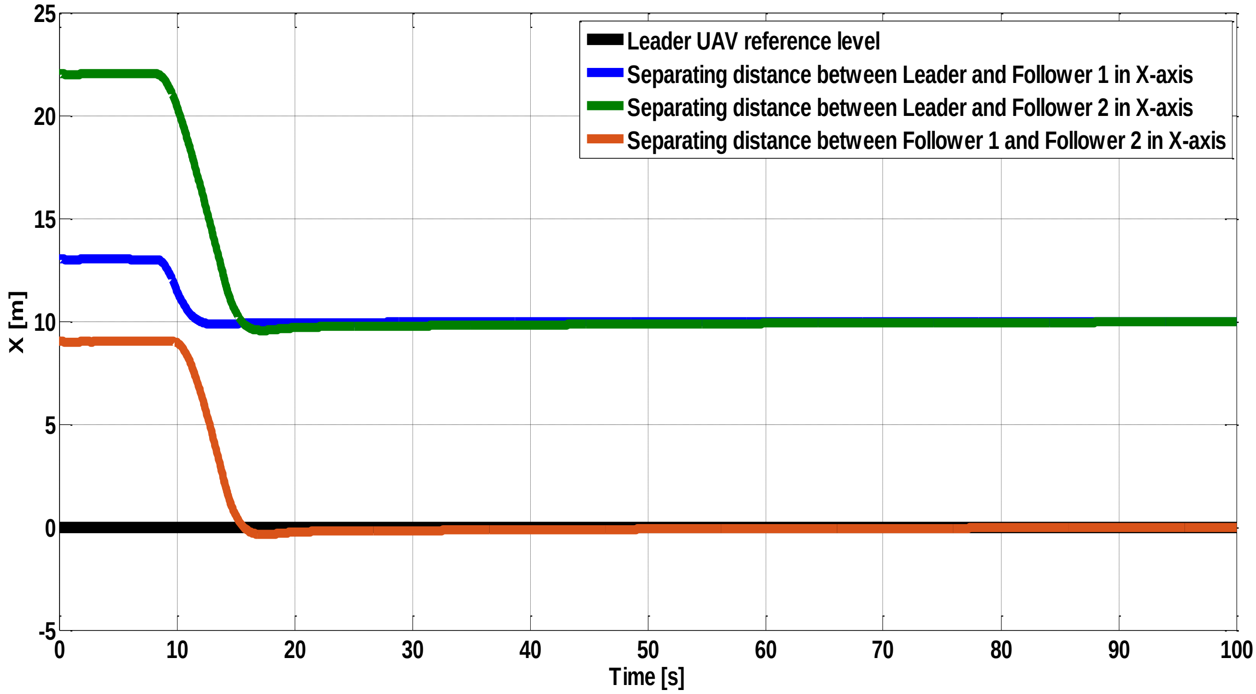

Fig. 7 Separating distance between the leader plane and its follower in X–axis.

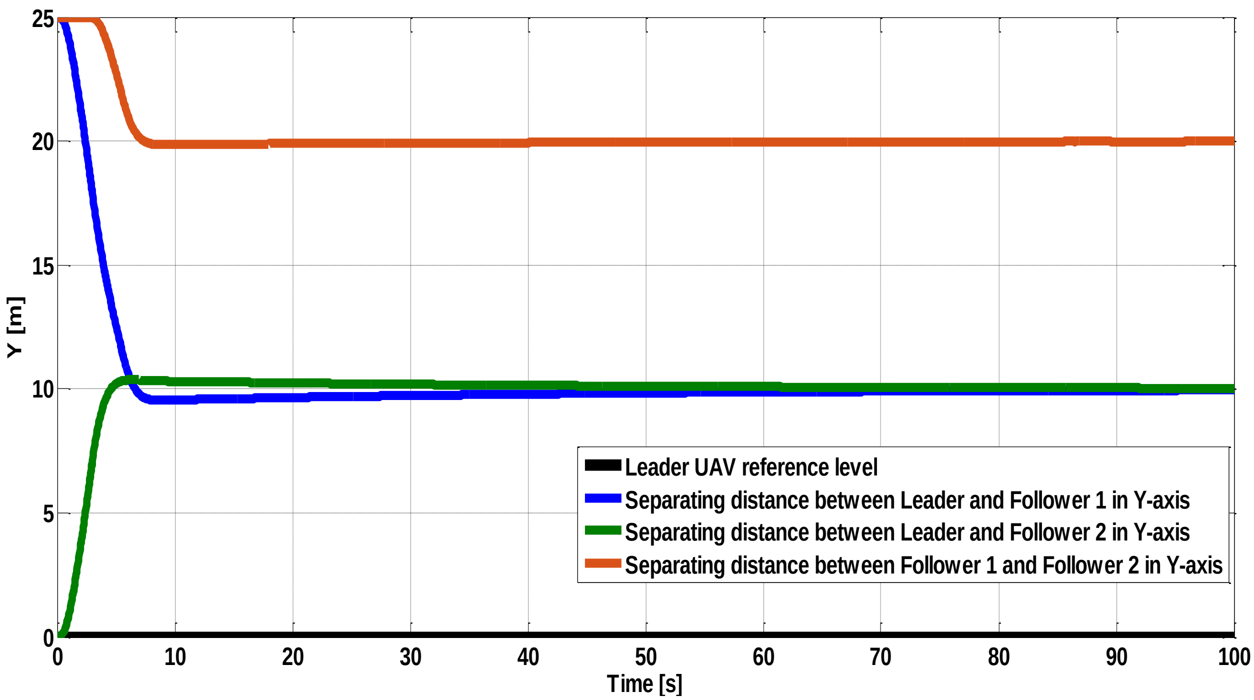

Fig. 8 Separating distance between the leader plane and its follower in Y-axis.

The controller succeeded to converge to the wanted detaching distance 10 m. V_x and V_y for the three quadrotors are represented in Fig. (9) and Fig. (10), respectively. The velocities converge within the desired value.

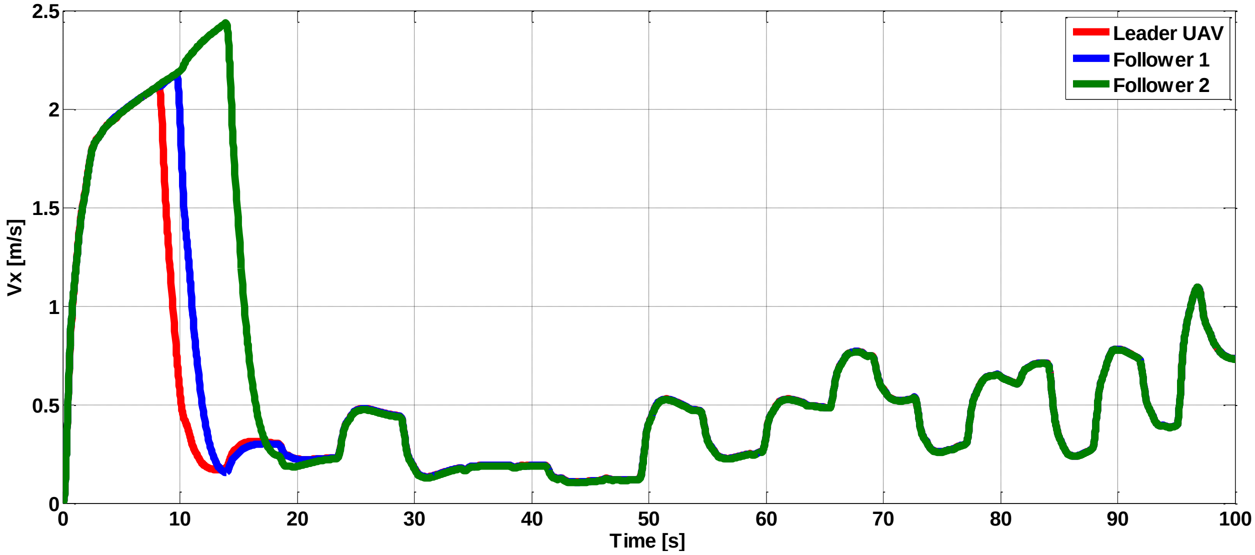

Fig. 9 Velocity control in X direction.

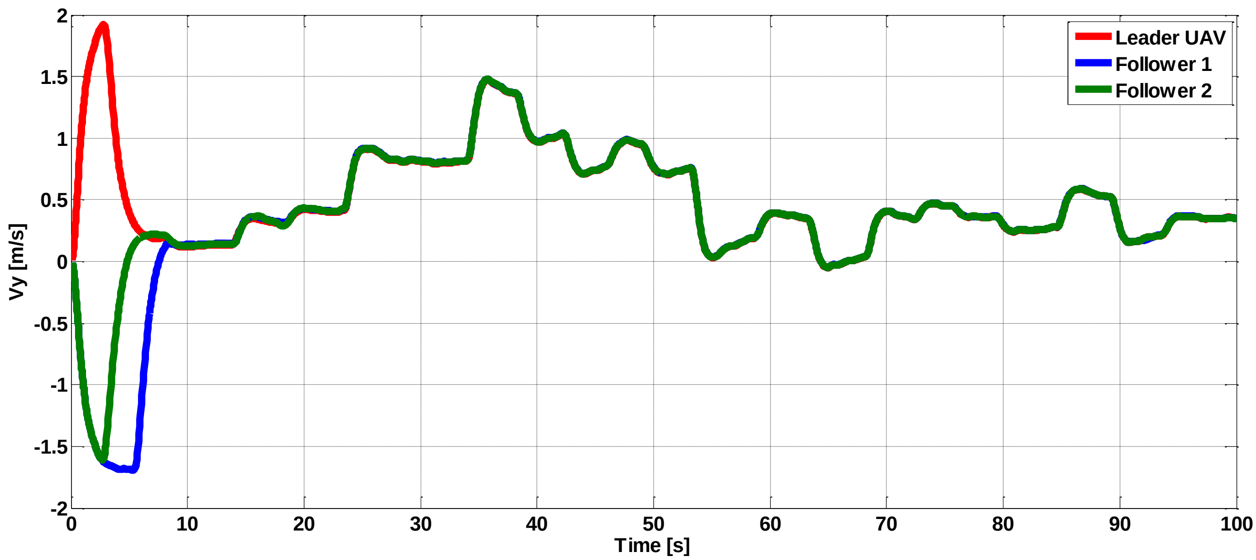

Fig. 10 Velocity control in Y direction.

Results from the simulation detained in the obstacle-free atmosphere, the designed controller achieves the desired path respecting the desired separating distances and velocities. One should notice that there is a slight difference between the responses of the two different kinds of paths. This difference between following step input path and parabolic path behaviors is due to slow rise time rate responding to the abrupt change. These responses can be accepted if compared with the attitude of the quadrotor in real-time flight. The cooperative quadrotors start initially from different operating points and converge to the desired positions respecting the constraints on the distance and velocity. The troop follows the designed trajectory and accomplishes their mission successfully.

B. An Obstacle-Loaded Atmosphere:

With a view to present the capacity of the underlying backstepping controller to pursue the desired trajectory in an obstacle-loaded atmosphere, obstacles were formed as a rectangle representing a plan view of an obstacle. For simplicity, the quadrotors altitudes were assumed as a constant height during the obstacle avoidance execution in the simulation. This would summarize the trajectory design complication to a 2D issue. For full flight safety reasons, a couple of security regions are constantly maintained with 20m-radius safety region and 10m-separating distance called protected region [61] between each follower of the troop and the leader plane respectively. These regions ensure a 20m-radius as a starting point to the troop to start the maneuver at the edge of this safety region between the troop members and any obstacle. If an obstacle is identified on the edge of the safety region, a security loop is activated causing trajectory tracking interruption and ensuring a dodgy maneuver in a half circle route to bypass the obstacle and then resume to complete the original trajectory as shown in Fig. 11.

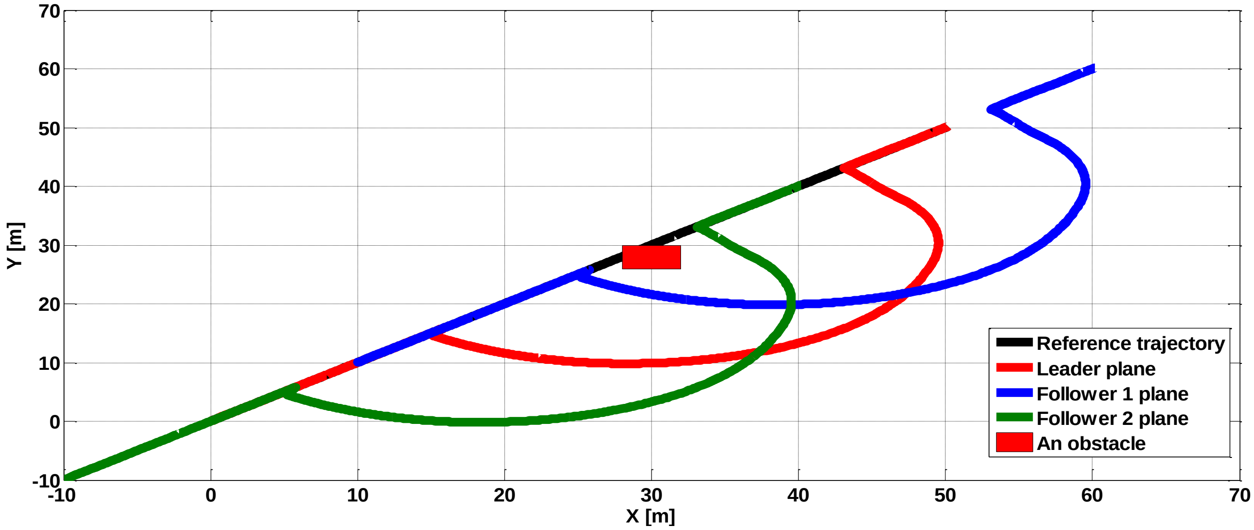

Fig. 11 The proposed obstacle avoidance algorithm of the quadrotors troop.

The method granted in this paper is a simple mathematical solution to the obstacle avoidance issue; this method identified the vertices and dimensions of the obstacles to avoid the collision. Let $x_{O\min}$ and $x_{O\max}$ represents the minimum and maximum ranges of the obstacle edges in x orientation. Similarly, $y_{O\min}$ and $y_{O\max}$ represents the minimum and maximum ranges of the obstacle edges in y orientation as highlighted in Fig. 12.

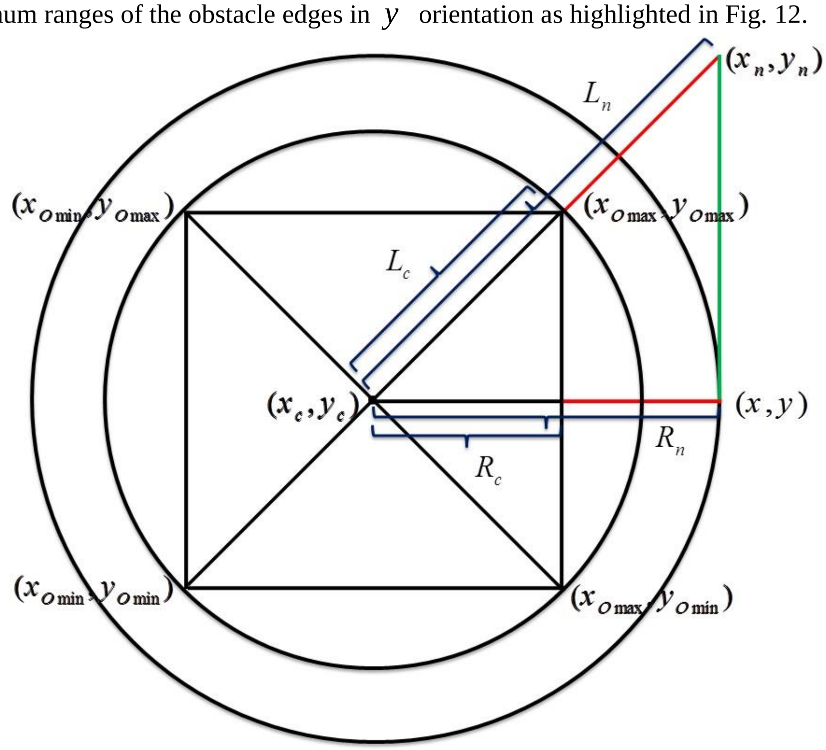

Fig. 12 A mathematical solution for the obstacle avoidance.

Let (x_c, y_c) the center point of the obstacle, so, the points can be obtained by equations (26, 27):

$$x_c = (x_{O\min} + x_{O\max})/2 \tag{26}$$

$$y_c = (y_{O\min} + y_{O\max})/2 \tag{27}$$

Assume the obstacle is cyclic quadrilateral, so, we can get the radius r_c of the circumscribed circle by:

$$r_c = 0.5 * \sqrt{(x_{O\max} - x_{O\min})^2 + (y_{O\max} - y_{O\min})^2} \tag{28}$$

By solving the drawn drawback mathematically, we can get the newly produced path from the series of (x, y) points of the trajectory path to a new series of (x_n, y_n) points after adding a safety distance s_d that enables the unmanned troop to avoid collision with the obstacle by:

$$x_n = x_c + (x - x_c) * r_c / s_d \tag{29}$$

$$y_n = y_c + (y - y_c) * r_c / s_d \tag{30}$$

The designed controller succeeded in controlling each unmanned quadrotor in the troop in a decentralized manner guaranteeing the reserving of the desired geometric formation as shown in Fig. 13.

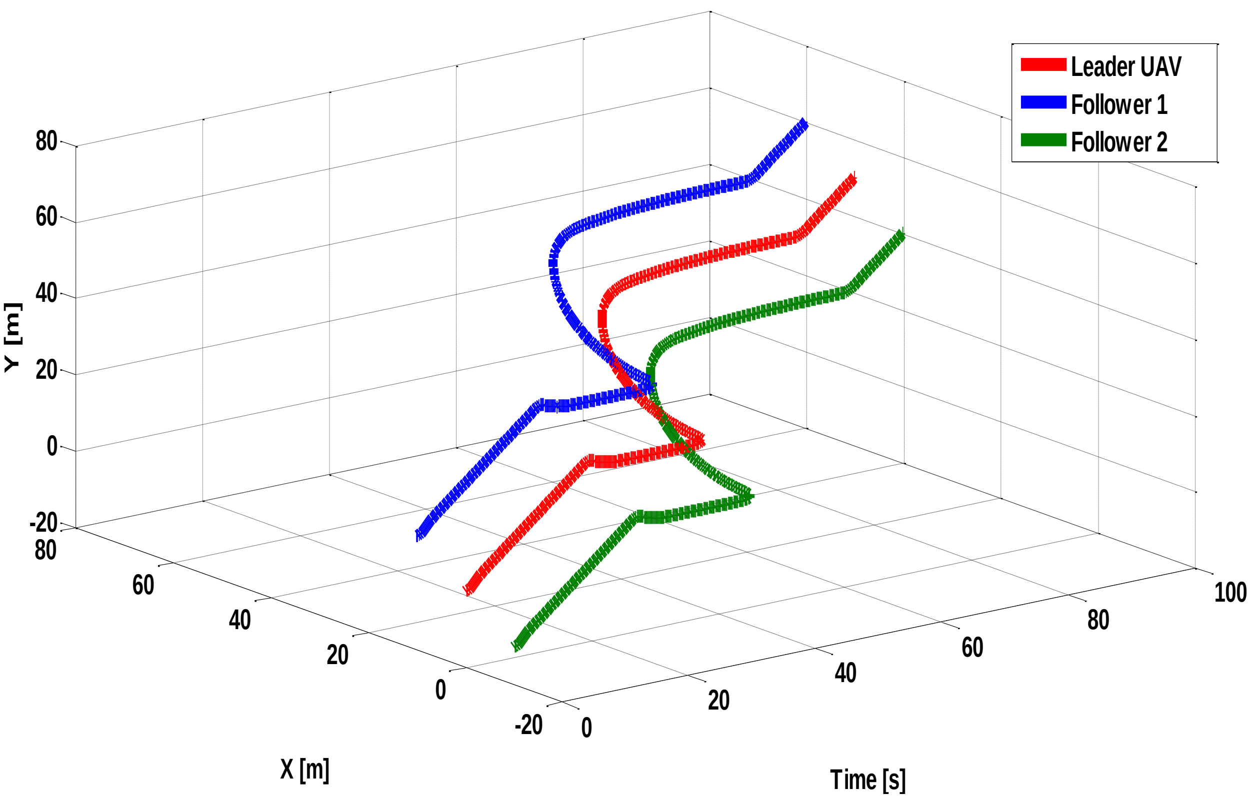

Fig. 13 The path of the quadrotors troop formation during avoiding the obstacle in 3-D.

The velocity of the leader in the X and Y pivots - V_x and V_y – are seen in Fig. 14, where the velocity converges to the allowable values after bypassing the obstacle.

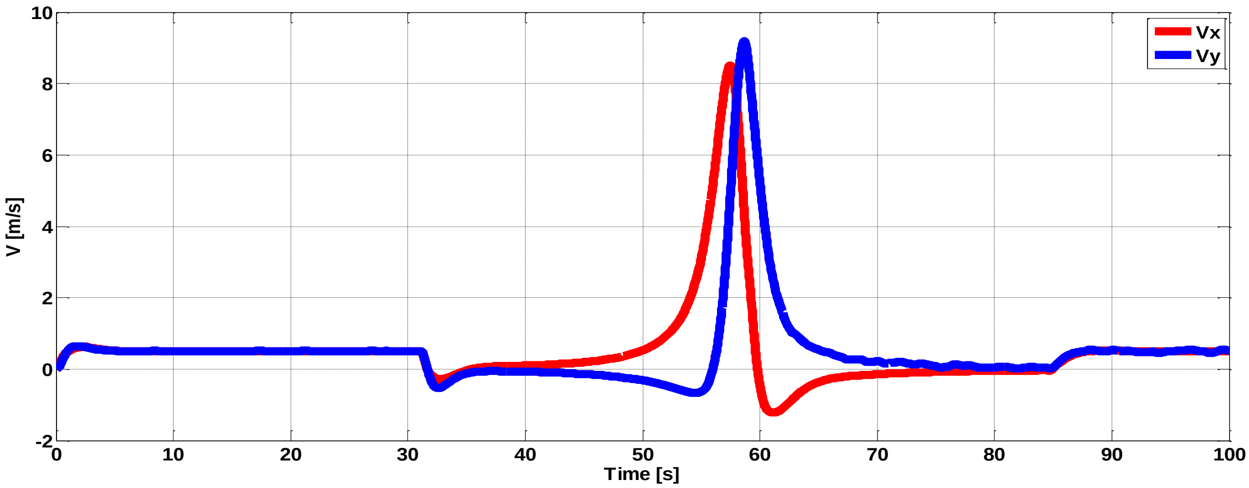

Fig. 14 Velocity control in X and Y orientations.

V. Conclusion

In this paper, backstepping PID controller is used to resolve the controversy of formation rearrangement for a troop of cooperative VTOL UAVs. The proposed controller is implemented to control each quadrotor of the troop in a decentralized way that guarantees stability and robustness of the complete formation of the troop. It can handle the under-actuated properties of the non linarites of each quadrotor. The simulation results show the effectiveness of the proposed controller in dealing with a cooperative unmanned VTOL air crafts in free or loaded obstacle atmosphere. The controller succeeded to UAV system to converge to the desired geometric formation either with existence or absence of obstacles.

In the future work, the proposed controller will be implemented and uploaded onboard quadrotors for real-time experiments. Also, new techniques such as adaptive neuro-fuzzy and self-adaptive PID will be applied to solve the formation problem for cooperative UAVs.

References

1. Hou, Z., et al. *A survey on the formation control of multiple quadrotors*. in *Ubiquitous Robots and Ambient Intelligence (URAI), 2017 14th International Conference on*. 2017: IEEE.
2. Min, Y.X., et al. *Formation tracking control of multiple quadrotors based on backstepping*. in *Control Conference (CCC), 2015 34th Chinese*. 2015: IEEE.
3. Madani, T. and A. Benallegue. *Backstepping control for a quadrotor helicopter*. in *Intelligent Robots and Systems, 2006 IEEE/RSJ International Conference on*. 2006: IEEE.
4. Pastor, E., J. Lopez, and P. Royo, *UAV payload and mission control hardware/software architecture.* IEEE Aerospace and Electronic Systems Magazine, 2007. **22**(6): p. 3-8.
5. Zheng, F.-y., H.-j. Gong, and Z.-y. Zhen, *Adaptive constraint backstepping fault-tolerant control for small carrier-based unmanned aerial vehicle with uncertain parameters.* Proceedings of the Institution of Mechanical Engineers, Part G: Journal of Aerospace Engineering, 2016. **230**(3): p. 407-425.
6. Özbek, N.S., M. Önkol, and M.Ö. Efe, *Feedback control strategies for quadrotor-type aerial robots: a survey.* Transactions of the Institute of Measurement and Control, 2015. **38**(5): p. 529-554.
7. Ren, W., *Multi-vehicle consensus with a time-varying reference state.* Systems & Control Letters, 2007. **56**(7): p. 474-483.
8. Hafez, A.T., et al., *Solving multi-UAV dynamic encirclement via model predictive control.* IEEE Transactions on control systems technology, 2015. **23**(6): p. 2251-2265.
9. Zhu, B., L. Xie, and D. Han. *Recent developments in control and optimization of swarm systems: A brief survey*. in *Control and Automation (ICCA), 2016 12th IEEE International Conference on*. 2016: IEEE.
10. Chen, J., et al., *Leader-follower formation control of multiple non-holonomic mobile robots incorporating a receding-horizon scheme.* The International Journal of Robotics Research, 2010. **29**(6): p. 727-747.

11. Marasco, A.J., *Control of cooperative and collaborative team tactics in autonomous unmanned aerial vehicles using decentralized model predictive control*. 2013: Library and Archives Canada= Bibliothq̀ue et Archives Canada.
12. Lazim, I.M., et al. *Optimal Formation Control of Multiple Quadrotors Based on Particle Swarm Optimization*. in *Asian Simulation Conference*. 2017: Springer.
13. Dudek, G., et al., *A taxonomy for multi-agent robotics.* Autonomous Robots, 1996. **3**(4): p. 375-397.
14. Zhang, Y. and H. Mehrjerdi. *A survey on multiple unmanned vehicles formation control and coordination: Normal and fault situations*. in *Unmanned Aircraft Systems (ICUAS), 2013 International Conference on*. 2013: IEEE.
15. Arrichiello, F., S. Chiaverini, and T.I. Fossen, *Formation control of marine surface vessels using the null-space-based behavioral control.* Group Coordination and Cooperative Control, 2006: p. 1-19.
16. Marasco, A.J., et al. *Dynamic encirclement of a moving target using decentralized nonlinear model predictive control*. in *American Control Conference (ACC), 2013*. 2013: IEEE.
17. Hafez, A.T., et al. *Task assignment/trajectory planning for unmanned vehicles via HFLC and PSO*. in *Unmanned Aircraft Systems (ICUAS), 2017 International Conference on*. 2017: IEEE.
18. Hafez, A. and S. Givigi. *Formation reconfiguration of cooperative UAVs via Learning Based Model Predictive Control in an obstacle-loaded environment*. in *Systems Conference (SysCon), 2016 Annual IEEE*. 2016: IEEE.
19. Reynolds, C.W., *An evolved, vision-based behavioral model of coordinated group motion.* From animals to animats, 1993. **2**: p. 384-392.
20. Iskandarani, M., et al. *Unmanned aerial vehicle formation flying using linear model predictive control*. in *Systems conference (syscon), 2014 8th annual ieee*. 2014: IEEE.
21. Rosales, C.D., et al. *Formation control of unmanned aerial vehicles based on the null-space*. in *Unmanned Aircraft Systems (ICUAS), 2014 International Conference on*. 2014: IEEE.
22. Wang, X., V. Yadav, and S. Balakrishnan, *Cooperative UAV formation flying with obstacle/collision avoidance.* IEEE Transactions on control systems technology, 2007. **15**(4): p. 672-679.
23. Bai, C., et al. *Dynamic multi-UAVs formation reconfiguration based on hybrid diversity-PSO and time optimal control*. in *Intelligent Vehicles Symposium, 2009 IEEE*. 2009: IEEE.
24. Duan, H., et al., *? Hybrid particle swarm optimization and genetic algorithm for multi-uav formation reconfiguration.* IEEE Computational intelligence magazine, 2013. **8**(3): p. 16-27.
25. Rajasree, R. and V. Jisha. *Optimal formation control of Unmanned Aerial Vehicles with reconfiguration*. in *Control Communication & Computing India (ICCC), 2015 International Conference on*. 2015: IEEE.
26. Hafez, A.T. and M.A. Kamel. *Fault-tolerant control for cooperative unmanned aerial vehicles formation via fuzzy logic*. in *Unmanned Aircraft Systems (ICUAS), 2016 International Conference on*. 2016: IEEE.
27. Ghamry, K.A. and Y. Zhang. *Fault-tolerant cooperative control of multiple UAVs for forest fire detection and tracking mission*. in *Control and Fault-Tolerant Systems (SysTol), 2016 3rd Conference on*. 2016: IEEE.
28. Liu, L., et al. *Distributed cooperative control for UAV swarm formation reconfiguration based on consensus theory*. in *Robotics and Automation Engineering (ICRAE), 2017 2nd International Conference on*. 2017: IEEE.
29. Zhang, H., W. Wang, and G. Xu. *Optimal control of formation reconfiguration for multiple UAVs based on Legendre Pseudospectral Method*. in *Control And Decision Conference (CCDC), 2017 29th Chinese*. 2017: IEEE.
30. Norouzi Ghazbi, S., et al., *QUADROTORS UNMANNED AERIAL VEHICLES: A REVIEW.* International Journal on Smart Sensing & Intelligent Systems, 2016. **9**(1).
31. Mahfouz, M. and S.A. Kader. *Quadrotor unmanned aerial vehicle controller design and synthesis*. in *Computer Engineering & Systems (ICCES), 2015 Tenth International Conference on*. 2015: IEEE.
32. Zhang, X., et al., *A Survey of Modelling and Identification of Quadrotor Robot.* Abstract and Applied Analysis, 2014. **2014**: p. 16.
33. Yu, Z., L. Feng, and H. Jie, *AMN-PSO METHOD FOR JAMMING UNMANNED AERIAL VEHICLE NETWORK.* International Journal on Smart Sensing & Intelligent Systems, 2015. **8**(4).
34. Guerrero, J.E., et al. *Preliminary design of a small-size flapping UAV. II. Aerodynamic Performance and Flight Stability*. in *XXI AIMETA Conference Book*. 2013.
35. Yu, G., H. Song, and J. Gao, *Unmanned aerial vehicle path planning based on TLBO algorithm.* International Journal on Smart Sensing and Intelligent Systems, 2014. **7**(3): p. 1310-1325.

36. Bouabdallah, S. and R. Siegwart. *Backstepping and sliding-mode techniques applied to an indoor micro quadrotor*. in *Robotics and Automation, 2005. ICRA 2005. Proceedings of the 2005 IEEE International Conference on*. 2005: IEEE.
37. Mahfouz, M., M. Ashry, and G. Elnashar, *Design and control of quad-rotor helicopters based on adaptive neuro-fuzzy inference system.* International Journal of Engineering Research Technology (IJERT), 2013. **2**: p. 479-485.
38. Raymer, D.P., *Aircraft design: a conceptual approach*. 2006: American Institute of Aeronautics and Astronautics Reston.
39. Rego, B.S., B.V. Adorno, and G.V. Raffo. *Formation Backstepping Control Based on the Cooperative Dual Task-Space Framework: A Case Study on Unmanned Aerial Vehicles*. in *Robotics Symposium and IV Brazilian Robotics Symposium (LARS/SBR), 2016 XIII Latin American*. 2016: IEEE.
40. Fethalla, N., et al. *Robust observer-based backstepping controller for a quadrotor UAV*. in *Electrical and Computer Engineering (CCECE), 2017 IEEE 30th Canadian Conference on*. 2017: IEEE.
41. Vallejo-Alarcón, M., R. Castro-Linares, and M. Velasco-Villa, *Unicycle-type robot & quadrotor leader-follower formation backstepping control.* IFAC-PapersOnLine, 2015. **48**(19): p. 51-56.
42. Davidi, A., N. Berman, and S. Arogeti. *Formation flight using multiple integral backstepping controllers*. in *Cybernetics and Intelligent Systems (CIS), 2011 IEEE 5th International Conference on*. 2011: IEEE.
43. Lee, K.U., Y.H. Choi, and J.B. Park, *Backstepping Based Formation Control of Quadrotors with the State Transformation Technique.* Applied Sciences, 2017. **7**(11): p. 1170.
44. Salierno, G.F. and G.V. Raffo, *WHOLE-BODY BACKSTEPPING CONTROL WITH INTEGRAL ACTION OF A QUADROTOR UAV.*
45. Basri, M.A.M., A.R. Husain, and K.A. Danapalasingam, *Nonlinear Control of an Autonomous Quadrotor Unmanned Aerial Vehicle using Backstepping Controller Optimized by Particle Swarm Optimization.* Journal of Engineering Science & Technology Review, 2015. **8**(3).
46. Liu, H., X. Wang, and H. Zhu. *A novel backstepping method for the three-dimensional multi-UAVs formation control*. in *Mechatronics and Automation (ICMA), 2015 IEEE International Conference on*. 2015: IEEE.
47. Basri, M., et al., *Design and optimization of backstepping controller for an underactuated autonomous quadrotor unmanned aerial vehicle.* Transactions of FAMENA, 2014. **38**(3): p. 27-44.
48. Qiu, L., et al. *Design of neural network and backstepping based adaptive flight controller for multi-effector UAV*. in *Robotics and Biomimetics (ROBIO), 2009 IEEE International Conference on*. 2009: IEEE.
49. Mian, A.A. and W. Daobo, *Modeling and backstepping-based nonlinear control strategy for a 6 DOF quadrotor helicopter.* Chinese Journal of Aeronautics, 2008. **21**(3): p. 261-268.
50. Li, Y. and S. Song. *A survey of control algorithms for quadrotor unmanned helicopter*. in *Advanced Computational Intelligence (ICACI), 2012 IEEE Fifth International Conference on*. 2012: IEEE.
51. Zhou, J. and C. Wen, *Adaptive backstepping control of uncertain systems: Nonsmooth nonlinearities, interactions or time-variations*. 2008: Springer.
52. Katsuhiko, O., *Modern control engineering*. 2010.
53. Ashry, M. *Comparative Study for Different Quad-Rotor Helicopter Feedback Controllers*. in *International Journal of Engineering Research and Technology*. 2014: ESRSA Publications.
54. Bang, H., J.-S. Lee, and Y.-J. Eun, *Nonlinear attitude control for a rigid spacecraft by feedback linearization.* Journal of Mechanical Science and Technology, 2004. **18**(2): p. 203-210.
55. Hamel, T., et al., *DYNAMIC MODELLING AND CONFIGURATION STABILIZATION FOR AN X4-FLYER.* IFAC Proceedings Volumes, 2002. **35**(1): p. 217-222.
56. Tayebi, A. and S. McGilvray, *Attitude stabilization of a VTOL quadrotor aircraft.* Control Systems Technology, IEEE Transactions on, 2006. **14**(3): p. 562-571.
57. Murray, R.M., et al., *A mathematical introduction to robotic manipulation*. 1994: CRC press.
58. Bouabdallah, S. and R. Siegwart. *Full control of a quadrotor*. in *Intelligent robots and systems, 2007. IROS 2007. IEEE/RSJ international conference on*. 2007: IEEE.
59. Bouabdallah, S., *Design and control of quadrotors with application to autonomous flying.* Lausanne Polytechnic University, 2007.
60. Wierema, M., *Design, implementation and flight test of indoor navigation and control system for a quadrotor UAV.* Master of Science in Aerospace Engineering at Delft University of Technology, 2008.
61. Mahjri, I., A. Dhraief, and A. Belghith. *A review on collision avoidance systems for unmanned aerial vehicles*. in *International Workshop on Communication Technologies for Vehicles*. 2015: Springer.